NJC

Accepted Manuscript

ROYAL SOCIETY OF CHEMISTRY

rsc.li/njc

View Article Online
DOI: 10.1039/C9NJ00061E

Copper(II) complexes based on tripodal pyridyl amine derivatives as efficient anticancer agents

Salah S. Massoud,[*a] Febee R. Louka,[a] Ada F. Tusa,[a] Nicole E. Bordelon,[a] Roland C. Fischer,[b] Franz A. Mautner,[*c] Ján Vančo,[d] Jan Hošek,[d] Zdeněk Dvořák[d] and Zdeněk Trávníček[*d]

[a] *Department of Chemistry, University of Louisiana at Lafayette, Lafayette, LA 70504, U. S. A.*

[b] *Institut für Anorganische Chemische, Technische Universität Graz, Stremayrgasse 9/V, A-8010 Graz, Austria*

[c] *Institut für Physikalische and Theoretische Chemie, Technische Universität Graz, Stremayrgasse 9/II, A-8010, Graz, Austria*

[d] *Division of Biologically Active Complexes and Molecular Magnets, Regional Centre of Advanced Technologies and Materials, Faculty of Science, Palacký University, Šlechtitelů 27, CZ-783 71 Olomouc, Czech Republic*

(Received: Accepted:)

Keywords Copper**;** Pyridyl compounds**;** Crystal structure**;** Anticancer activity**;** Cytotoxicity

Electronic supplementary information (ESI) available. CCDC-1885301-1885307 contain the crystallographic data in CIF format for **2-PF_6**, **4-ClO_4**, **4-PF_6**, **5-PF_6**, **7-ClO_4**, **8-ClO_4** and **6-PF_6**, respectively. These data can be obtained free of charge from The Cambridge Crystallographic Data Centre via www.ccdc.cam.ac.uk/data_request/cif. Selected bond and angles are summarized in Table S1. ESI materials associated with the gel electrophoresis results (Figs S1-S6) of this article can be found, in the online version at http://dx.doi.org/??????????????????????.

* Corresponding authors: E-mail: ssmassoud@louisiana.edu, Tel. +01 337-482-5672, Fax: +01 337-482-5676 (S.S. Massoud); E-mail: mautner@tugraz.at, Tel. ++43 316-873-32270, Fax: ++43 316-873-8225 (F.A. Mautner); E-mail: zdenek.travnicek@upol.cz, Tel. +420 585-634-352, Fax: +420 585-634-954 (Z. Trávníček).

View Article Online
DOI: 10.1039/C9NJ00061E

Abstract

The complexes [Cu(TPA)Cl]ClO_4.½H_2O (**1-ClO_4**), [Cu(6-MeTPA)Cl]ClO_4/PF_6 (**2-ClO_4/2-PF_6**), [Cu(6-Me_2TPA)Cl]PF_6 (**3-PF_6**), [Cu(BPQA)Cl]ClO_4/PF_6 (**4-ClO4/4-PF_6**), [Cu(BPQA)Cl]ClO_4/PF_6 (4- **ClO_4/4-PF_6**), [Cu(BQPA)Cl]ClO_4/PF_6 (**5-ClO_4/PF_6**), [Cu(L^1)Cl]ClO_4/PF_6 (**6-ClO_4/6-PF_6**), [Cu(L^2)Cl]ClO_4 (**7-ClO_4**) and [Cu(L^3)Cl]ClO_4 (**8-ClO_4**) have been synthesized and structurally characterized by spectroscopic techniques and single X-ray crystallography. The *in vitro* cytotoxicity of the prepared Cu(II) complexes were evaluated against A2780 (ovarian), A2780R (cisplatin-resistant variant) and MCF7 (breast cancer) human cancer cell lines. Overall, the complexes revealed significant-to-moderate cytotoxicity, with the best results obtained for the complexes [Cu(BQPA)Cl]ClO_4 (**5-ClO_4**) and [Cu(BQPA)Cl]PF_6 (**5-PF_6**) showing IC_{50} values within the range of 4.7–10.8 μM. The ability of the most cytotoxic complexes to cleave the DNA at different conditions and the mechanisms underlying this activity were assessed by means of the agarose gel electrophoresis.

View Article Online
DOI: 10.1039/C9NJ00061E

Introduction

According to **W**orld **H**ealth **O**rganization cancer is considered as the second most common cause of death worldwide after cardiovascular diseases. In 2015, cancer diseases were responsible for 8.8 million deaths around the world. Sadly, this figure is expected to rise to 15.1 million people in 2030.[1,2] Moreover, in the developed countries, it was statistically pointed out that two in every five born people will be diagnosed with cancer during their life time. The mortality data which were collected in 2016 by the National Center for Health Statistics predicted 1,685,210 new cancer cases and 595,690 cancer deaths were projected to occur in the United States.[1,2]

In the design of anticancer agents, the transition metal complexes provide some interesting properties which may not exist in the organic compounds. These include the nature of the central metal ion, its coordination number, oxidation state, redox properties, the geometry of the coordination compound, its thermodynamic and kinetic stability as well as the wide variety in the co-ligand(s) skeleton coordinated to the central metal ion. The great success of cisplatin and the second and third generation of its derivatives, used as clinically effective therapeutic agents in the fight against a wide spectrum of cancers,[3,4] was confronted by some major problems associated with the serious side effects of these drugs and the resistance exhibited by some cancer cells.5 Extensive attempts have been directed into this area to develop alternative therapeutic agents that can improve the effectivity (i.e. cytotoxicity against cancer cells) of the drug, while reducing its dose and its toxicity.[4] Many metal complexes, derived from ruthenium(II/III), gold(I/III), gallium(III), titanium((III/IV), iron(II/III) and cobalt(II/III) with a variety of ligand structures, have been launched and investigated as anticancer therapeutic agents.[6-11]

In the search for developing of effective antitumor agents copper(I/II) complexes constructed from polydentate linear, Schiff bases, macrocycles or tripodal-tetradentate ligands with *X-donor* atoms (X = N; O; S; N, O; N, O, S) were designed and tested for their anticancer activities against different human cancer cell lines such as MCF7 (breast cancer), A2780 (ovarian), A2780R (cisplatin-resistant variant), HOS (aggressive bone tumors), CaCo2 (epithelial colorectal adenocarcinoma), AS49 (lung), DU-145 (prostate), HCT-15 (Colon), HeLa (human cervix epithelial carcinoma) and hepatocytes.[12-35] There are also some recent review papers taking together the knowledge about the anticancer activities and the underlying mechanisms of action regarding the copper complexes. [6,12, 13] Copper complexes were introduced into this area based on the assumption that as it is an essential element for life, it may be less toxic compared to other used metal complexes.[5,12,13,35] Copper plays a

View Article Online
DOI: 10.1039/C9NJ00061E

crucial role not only in biochemistry but also in medicine.[5,12,36] In contrast, while the metal has been used in the treatment of copper deficiency in Menkes disease, excess copper should be removed from the body with a chelating therapeutic agents in Wilson disease.[5,12,36]

Recently, a series of copper(II) complexes with tripodal tris(pyridin-2-yl)amine ligands were investigated for their *in vitro* anticancer potential against some tumor cell lines.[26] This study did not reveal any systematic behavior between the pyridyl copper compounds and the observed cancer activity.[26] However, this result motivated us to perform a screening focused on the effect of substituents in the parent tris(2-pyridylmethyl)amine (TPA) ligand (Scheme 1) and the *in vitro* cytotoxicity of their corresponding Cu(II) complexes, $[Cu(L)X]ClO_4/PF_6$ (L = any ligand shown in Scheme 1), against some cancer cells in order to evaluate their cytotoxic effectiveness compared to the standard *cisplatin*.

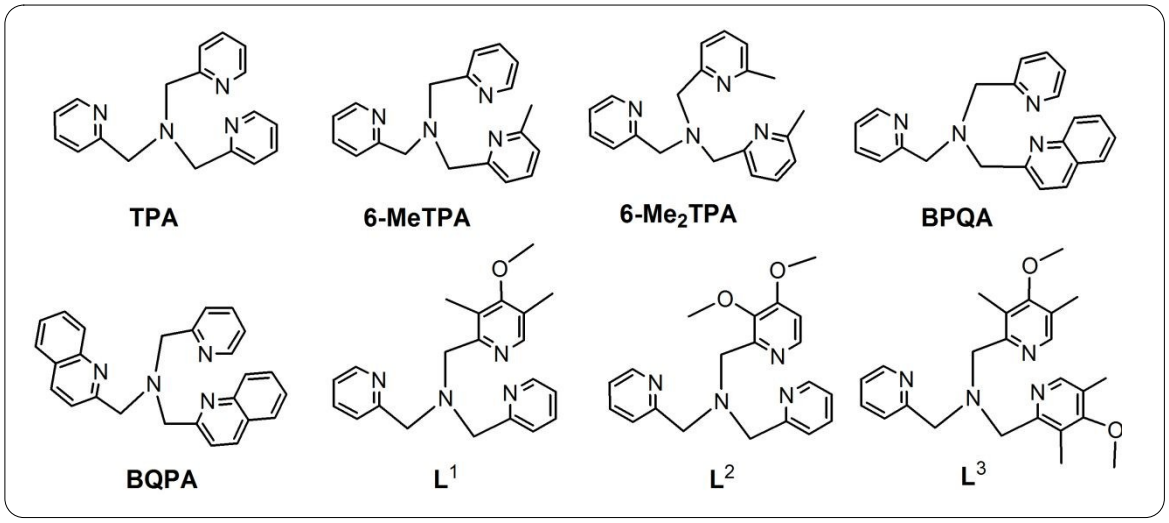

Scheme 1 Structural formulas of the tripod pyridyl-based ligands used in this study.

Results and discussion

Synthetic aspects

The tripod tetradentate *N*-donor atoms based pyridyl groups, shown in scheme 1 (6-MeTPA, 6-Me_2TPA, BPQA, BQPA, L^1, L^2 and L^3), with the exception of TPA,[37,38] were synthesized by gentle reflux and stirring (48-72 h) of a slurry mixture containing 2-aminomethylpyridine or di(2-pyridyl)amine with the appropriate 2-chloromethylpyridine hydrochloride derivatives or 2-chloromethylquinoline hydrochloride under anhydrous conditions of CH_3CN or THF in the presence

View Article Online
DOI: 10.1039/C9NJ00061E

of anhydrous Na_2CO_3/Cs_2CO_3 or Et_3N, which is used in slight excess used more than the stoichiometric amounts under nitrogen.[39,40] These compounds, which solidified upon standing at room temperature require several recrystallization from Et_2O with the aid of activated charcoal were characterized by elemental microanalysis, IR, ^1H and ^{13}C NMR spectroscopy as well by ESI-MS.

The syntheses of the chlorido copper(II) complexes: $[Cu(TPA)Cl]ClO_4.½H_2O$ (**1-ClO$_4$**),[41] $[Cu(6\text{-}MeTPA)Cl]ClO_4$ (**2-ClO$_4$**), $[Cu(6\text{-}MeTPA)Cl]PF_6$ (**2-PF$_6$**), $[Cu(6\text{-}Me_2TPA)Cl]PF_6$ (**3-PF$_6$**), $[Cu(BPQA)Cl]ClO_4$ (**4-ClO4**), $[Cu(BPQA)Cl]PF_6$ (**4-PF$_6$**), $[Cu(BQPA)Cl]ClO_4$ (**5-ClO$_4$**), $[Cu(BQPA)Cl]PF_6$ (**5-PF$_6$**), $[Cu(L^1)Cl]PF_6$ (**6-PF$_6$**), $[Cu(L^1)Cl]ClO_4$ (**6-ClO$_4$**), $[Cu(L^2)Cl]ClO_4$ (**7-ClO$_4$**) and $[Cu(L^3)Cl]ClO_4$ (**8-ClO$_4$**) were achieved by the reaction of a methanolic solution of the ligand and $CuCl_2.2H_2O$ in a 1:1 molar ratio, followed by addition of slight excess of $NaClO_4$ or NH_4PF_6. The isolated complexes, were crystallized from CH_3CN to remove the chloride salt and unreacted $NaClO_4$/NH_4PF_6. In most cases further recrysallization of the products from MeOH resulted in the isolation of single crystals of suitable for X-ray structure determination. These complexes which were produced in pure form with reasonable to good yields (51-93%) were characterized by elemental microanalyses, molar conductivity measurements, IR, UV-Vis and single crystal X-ray crystallography as well as by ESI-MS in some cases.

Description of the crystal structures

The structures of the seven complexes: **2-PF$_6$**, **4-PF$_6$**, **4-ClO$_4$**, **5-PF$_6$**, **6-PF$_6$**, **7-ClO$_4$** and **8-ClO$_4$** were determined and selected interatomic parameters in the vicinity of the Cu(II) centers are listed in Table 1. In these complexes, the copper(II) centers of the mononuclear complex cations are penta-coordinated by four *N*-donor atoms of the tripod tetraamine ligand and one terminal chloride anion as illustrated in Fig. 1. The CuN_4Cl chromophores form distorted trigonal bipyramids (TBP) in **5-PF$_6$**, **6-PF$_6$**, **7-ClO$_4$** and **8-ClO$_4$** with τ-values of 0.64, 0.96 (mean), 0.86 and 0.80, respectively (τ-values of 0 and 1 refer to ideal geometries of square pyramid (SP) and trigonal bipyramid, respectively).[42] The axial sites are occupied by terminal chloride anion and N(amine), whereas the three equatorial sites are occupied by the three pyridyl nitrogen donor atoms. In **2-PF$_6$**, **4-PF$_6$**, **4-ClO$_4$** the CuN_4Cl chromophores form distorted square pyramids with τ-values of 0.12, 0.16, and 0.13, respectively. The Cu-Cl bond distances vary from 2.222 to 2.2528 Å, the Cu-N(amine) from 2.004 to 2.0612 Å, and the Cu-N(pyridyl) from 1.9831 to 2.3616 Å. For the CuN_4Cl chromophores in penta-coordinated

View Article Online
DOI: 10.1039/C9NJ00061E

[Cu(TPA)Cl]$ClO_4 \cdot ½H_2O$ (**1-ClO$_4$**), [Cu(6-MeTPA)Cl]ClO_4 (**2-ClO$_4$**) and [Cu(6-Me$_2$TPA)Cl]ClO_4 (**3-ClO$_4$**) τ-values of 0.98 and 0.94; 0.16 and 0.24; 0.07, respectively, were reported.[41,43]

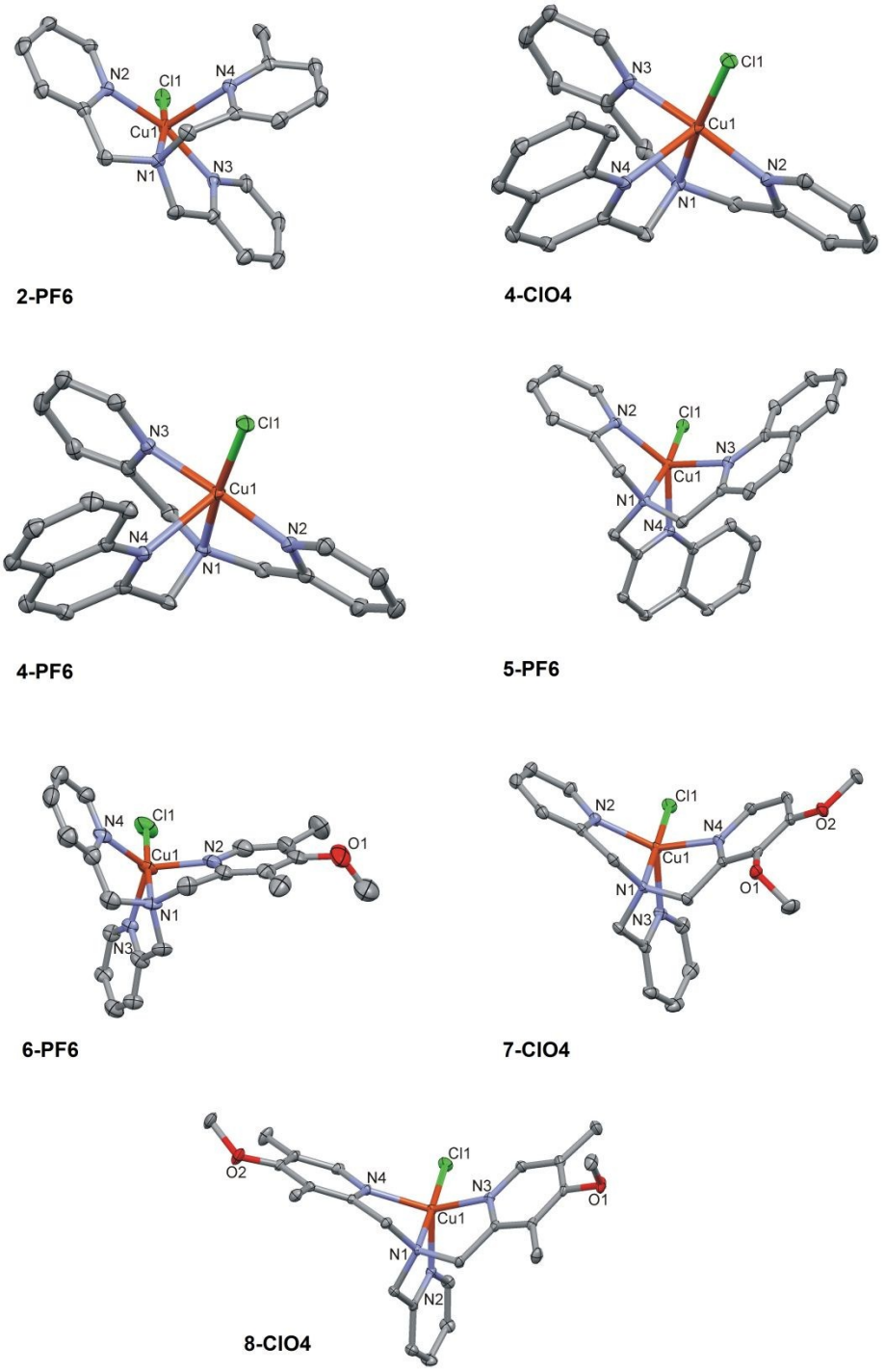

Fig. 1 Representative plots of coordination spheres of **2-PF$_6$**, **4-PF$_6$**, **4-ClO$_4$**, **5-PF$_6$**, **6-PF$_6$**, **7-ClO$_4$** and **8-ClO$_4$** together with partial atom numbering scheme.

View Article Online
DOI: 10.1039/C9NJ00061E

Table 1 Selected bond distances (Å) and bond angles (°) of **2-PF_6**, **4-ClO_4** and **4-PF_6**

	2-PF_6	**4-ClO_4**	**4-PF_6**
Cu1-N2	1.9885(16)	1.9934(12)	1.9831(13)
Cu1-N3	2.0026(16)	2.0099(12)	2.0034(13)
Cu1-N4	2.3616(16)	2.3572(12)	2.3473(14)
Cu1-N1	2.0585(16)	2.0612(11)	2.0606(12)
Cu1-Cl1	2.2480(5)	2.2528(4)	2.2453(4)
N1-Cu1-Cl1	170.48(5)	172.00(3)	170.82(4)
N2-Cu1-N3	162.86(7)	162.57(5)	163.03(5)
N2-Cu1-N4	100.46(6)	101.92(4)	100.46(5)
N3-Cu1-N4	86.04(6)	83.90(4)	85.12(5)
τ-value	0.119	0.157	0.130

Table 1 Cont. Selected bond distances (Å) and bond angles (°) of **5-PF_6**, **7-ClO_4** and **8-ClO_4**

	5-PF_6	**7-ClO_4**	**8-ClO_4**
Cu1-N2	2.0733(9)	2.0291(17)	2.1022(12)
Cu1-N3	2.2512(9)	2.0973(18)	2.0394(12)
Cu1-N4	2.1115(9)	2.0542(17)	2.0464(12)
Cu1-N1	2.0251(9)	2.0505(16)	2.0317(12)
Cu1-Cl1	2.2264(3)	2.2250(5)	2.2411(4)
N1-Cu1-Cl1	171.07(3)	179.65(5)	178.34(4)
N2-Cu1-N3	114.50(3)	122.48(7)	113.44(5)
N2-Cu1-N4	132.69(4)	128.22(7)	109.12(5)
N3-Cu1-N4	103.41(3)	103.11(7)	130.64(5)
τ-value	0.640	0.857	0.795

Table 1 Cont. Selected bond distances (Å) and bond angles (°) of **6-PF_6**.

	6-PF_6		·
Cu1-N2	2.049(4)	Cu2-N8	2.045(4)
Cu1-N3	2.072(5)	Cu2-N7	2.074(5)

View Article Online
DOI: 10.1039/C9NJ00061E

Cu1-N4	2.067(5)	Cu2-N6	2.047(5)
Cu1-N1	2.022(4)	Cu2-N5	2.042(4)
Cu1-Cl1	2.2386(18)	Cu2-Cl2	2.2384(15)
N1-Cu1-Cl1	177.40(14)	N5-Cu2-Cl2	178.01(14)
N2-Cu1-N4	121.8(2)	N6-Cu1-N7	119.2(2)
τ-value	0.927	τ-value	0.980
Cu3-N9	2.043(5)	Cu4-N13	2.031(5)
Cu3-N11	2.098(5)	Cu4-N15	2.062(5)
Cu3-N12	2.029(4)	Cu4-N16	2.073(5)
Cu3-N10	2.046(5)	Cu4-N14	2.092(3)
Cu3-Cl3	2.2399(16)	Cu4-Cl4	2.2124(18)
N9-Cu3-Cl3	178.65(14)	N13-Cu4-Cl4	178.15(16)
N10-Cu3-N12	121.56(19)	N15-Cu4-N14	118.75(16)
τ-value	0.952	τ-value	0.990

Characterization of the compounds

The acetonitrile molar conductivity of the chlorido-Cu(II) complexes under investigation gave Λ_M values in the range of 137 to 149 $\Omega^{-1}cm^2mol^{-1}$ which are typical for 1:1 electrolytic behavior.[44] The ESI-MS of the complexes **2-ClO$_4$** and **8-ClO$_4$** in CH_3CN revealed the presence of the molecular ion $[Cu(L)Cl]^+$, where L = MeTPA or L^3, respectively with perfect agreement between the calculated and experimental *m/z* values (see experimental section). Similar results were produced for corresponding counter anions ClO_4^- or PF_6^-.

The ATR-IR spectra of complex **1-ClO$_4$**, **4-ClO$_4$**, **5-ClO$_4$**, **6-ClO$_4$**, **7-ClO$_4$** and **8-ClO$_4$** display a very strong band at 1074-1093 cm^{-1}, which is assigned to stretching vibration of ν(Cl-O) of the perchlorate counter ion. The split for this band into 1114 and 1093 cm^{-1} in the later complex is most likely attributed to the distortion of the perchlorate counter ion and reducing its symmetry from T_d to C_{3v} or C_{2v}. On the other hand, the hexafluoroammonium phosphate compounds **3-PF$_6$** , **4-PF$_6$**, **5-PF$_6$**

View Article Online
DOI: 10.1039/C9NJ00061E

and **6-PF_6** revealed a strong band over the vibration range 827-854 cm^{-1} due to ν(P-F) of the PF_6^- counter ion. The very weak bands observed above 3000±100 cm^{-1} are attributed to the ν(C-H) strtching vibration, of the pyridyl/quinoly and the aliphatic C-H vibrations, respectively. Whereas, the medium to weak intensity vibrational band over the range 1610-1400 cm^{-1} are characteristic to the pyridyl moieties.[38-41]

Table 2 The UV-Vis spectral and molar conductivity, Λ_M data of the complexes under investigation in CH_3CN solutions.

Complex	**UV-Vis** λ_{max}, nm (ε_{max} , $M^{-1}cm^{-1}$)	**Assigned Geometry** (dist TBP *vs* SP) [a]	**Λ_M** ($\Omega^{-1}cm^2mol^{-1}$)
$[Cu(TPA)Cl]ClO_4 \cdot ½H_2O$ [b] (**1-ClO_4**)	~730 (sh), 950 (b)	dist TBP	177 [c]
$[Cu(6\text{-}MeTPA)Cl]ClO_4$ (**2-ClO_4**)	~660 (sh), 900 (112, b)	dist TBP	142
$[Cu(6\text{-}MeTPA)Cl]PF_6$ (**2-PF_6**)	~670 (sh), 885 (132, b)	dist TBP	143
$[Cu(6\text{-}Me_2TPA)Cl]PF_6$ (**3-PF_6**)	685 (148), ~860 (sh)	dist SP	146
$[Cu(BPQA)Cl]ClO_4$ (**4-ClO_4**)	~640, 880 (151, b)	dist TBP	141
$[Cu(BPQA)Cl]PF_6$ (**4-PF_6**)	~700 (sh), 900 (159, b)	dist TBP	147
$[Cu(BQPA)Cl]ClO_4$ (**5-ClO_4**)	730 (138, b), ~880 (143, b)	intermediate	145
$[Cu(BQPA)Cl]PF_6$ (**5-PF_6**)	~660 (sh), 880 (141, b)	dist TBP	146
$[Cu(L^1)Cl]ClO_4$ (**6-ClO_4**)	~725 (sh), 955 (221)	dist TBP	143
$[Cu(L^1)Cl]PF_6$ (**6-PF_6**)	~700 (sh), ~ 850 (sh), 970 (355)	dist TBP	147
$[Cu(L^2)Cl]ClO_4$ (**7-ClO_4**)	~715 (sh), 960 (230, b)	dist TBP	149
$[Cu(L^3)Cl]ClO_4$ (**8-ClO_4**)	~710 (sh), ~880 (sh), 970 (371)	dist TBP	137

[a] dist = distorted, TBP = trigonal bipyramid, SP = square pyramid
[b] Ref 41
[c] Determined in aqueous solution

The visible spectra of the complexes in CH_3CN are summarized in Table 2 together with their molar conductivity. Inspection of this data reveal that the complexes have similar spectral features. With the exception of **3-PF_6**, the complexes in general exhibit a shoulder over the wavelength range (640-730 nm) and a broad band at $\lambda_{max} \geq 850$ nm.[45] These spectral features are fully consistent with *five-coordinate* species with distorted trigonal bipyramidal geometry (TBP) around the central Cu(II) ion. In contrast, the more sterically hindered complex $[Cu(6\text{-}Me_2TPA)Cl]PF_6$ (**3-PF_6**) showed an intense broad band at 685 and a shoulder at around 860 nm where this feature is in an agreement with a distorted square pyramidal geometry (SP). On the other hand, the appearance of two broad bands

View Article Online
DOI: 10.1039/C9NJ00061E

around 730 and 880 nm of almost the same intensity in [Cu(BQPA)Cl]ClO_4 (**5-ClO_4**) may indicate an intermediate geometry between TBP and SP around the central Cu(II) ion with a slightly increased distortion towards SP geometry.[45-49] The TBP geometrical assignments in acetonitrile solution were in full agreements with those obtained from X-ray structural determinations in complexes **5-PF_6**, **6-PF_6**, **7-ClO_4** and **8-ClO_4**, whereas the complexes **2-PF_6**, **4-PF_6** and **4-ClO_4** revealed a pronounced tendency toward SP geometry in the solid state (see X-ray section).

Solution studies of the complexes

The visible spectra of the complexes under investigation in CH_3CN, CH_3OH and aqueous acetonitrile solutions produced the same spectra and did not show any sign of spectral changes over a period of five days. Moreover, the molar conductivities of the complexes in these media and over the tested time period were eventually unchanged within the experimental error and fully consistent with 1:1 electrolyte ($[Cu(L)Cl]^+ + ClO_4^-/PF_6^-$) as determined before in CH_3CN solution. These indicate that the complexes in these media are very stable and do not undergo any hydrolysis and/or solvolysis reactions as well as their configurations are retained in these media as the chlorido, $[Cu(L)Cl]^+$ complex ion. The corresponding Co(II) complexes, [Co(L)Cl]ClO_4/PF_6 with L = TPA, 6-MeTPA, 6-Me_2TPA, BPQA, BQPA, L^1, L^2 and L^3, were reported to undergo aquation and/or solvolysis through the chloride displacement reactions ($[Co(L)(H_2O/CH_3CN)]^{2+}$) and this process was accompanied by dramatic color, spectral and conductivity changes.[39,40]

In vitro cytotoxicity

The *in vitro* cytotoxicity of the complexes against a series of human cancer cell lines (A2780, A2780R and MCF7) was studied using the MTT cell viability assay. The cytotoxicity of the complexes under investigation together with cisplatin used as a reference drug was evaluated under the same experimental conditions. The IC_{50} values, calculated from the dose-survival curves obtained after 24 h incubation with the complexes, are shown in Table 3.

View Article Online
DOI: 10.1039/C9NJ00061E

Table 3 The cytotoxicity of the studied complexes and *cisplatin* against a series of human cancer cell lines (ovarian cancer A2780, ovarian cancer resistant to cisplatin A2780R, and breast adenocarcinoma MCF7). The values of half maximal inhibitory concentration (IC_{50}) of cells viability were calculated from the corresponding dose-response curves.

Complex		A2780	A2780R	MCF7
$[Cu(TPA)Cl]ClO_4 \cdot ½H_2O$	(**1-ClO$_4$**)	> 100	Not tested	52.3 ± 1.4
$[Cu(6\text{-}MeTPA)Cl]ClO_4$	(**2-ClO$_4$**)	83.2 ± 2.1	> 100	23.7 ± 0.6
$[Cu(6\text{-}MeTPA)Cl]PF_6$	(**2-PF$_6$**)	23.2 ± 2.5	> 100	57.9 ± 4.5
$[Cu(6\text{-}Me_2TPA)Cl]PF_6$	(**3-PF$_6$**)	21.1 ± 3.3	54.2 ± 1.9	17.4 ± 0.4
$[Cu(BPQA)Cl]ClO_4$	(**4-ClO$_4$**)	18.2 ± 3.0	28.5 ± 3.0	25.9 ± 3.0
$[Cu(BPQA)Cl]PF_6$	(**4-PF$_6$**)	20.5 ± 1.0	47.3 ± 0.5	29.2 ± 1.3
$[Cu(BQPA)Cl]ClO_4$	(**5-ClO$_4$**)	4.9 ± 0.8	9.4 ± 1.1	5.5 ± 0.3
$[Cu(BQPA)Cl]PF_6$	(**5-PF$_6$**)	4.7 ± 0.1	8.0 ± 2.0	10.8 ± 0.3
$[Cu(L^1)Cl]ClO_4$	(**6-ClO$_4$**)	23.6 ± 3.7	36.7 ± 1.1	31.9 ± 3.1
$[Cu(L^1)Cl]PF_6$	(**6-PF$_6$**)	28.5 ± 4.0	36.2 ± 2.8	31.0 ± 0.6
$[Cu(L^2)Cl]ClO_4$	(**7-ClO$_4$**)	81.7 ± 5.6	> 100	26.9 ± 2.7
$[Cu(L^3)Cl]ClO_4$	(**8-ClO$_4$**)	11.3 ± 0.8	> 100	25.5 ± 2.1
cisplatin		15.7 ± 1.8	> 50	21.5 ± 0.5

Complexes **5-ClO$_4$** and **5-PF$_6$** showed the best cytotoxicity against all three cancer cell lines, significantly better than that of the reference *cisplatin*. Moreover, the cytotoxic effects of these complexes were not influenced by the intrinsic resistance of A2780R cell line against *cisplatin*, which might indicate that another mechanism of action (as compared with *cisplatin*) is responsible for this biological activity. These two complexes are about three times more effective than *cisplatin* towards A2780, and they also revealed significant effectiveness against A2780R and MCF7 cancer cells. . The cytotoxicity of **4-ClO$_4$** and **4-PF$_6$** compounds is comparable to that observed for cisplatin. Overall, it may be concluded that the complexes revealed significant-to-moderate cytotoxicity against the human cancer cell lines used. These results are comparable with previously reported cytotoxicity data obtained for copper(II) complexes involving tris(pyridin-2-yl-alkyl)amine ligands.[26] In both cases, the complexes differed in their counter-ions only (ClO_4^- *vs.* PF_6^-), which in most cases do not have a substantial impact on the resulting cytotoxicity of the complexes, as previously demonstrated.[50]

View Article Online
DOI: 10.1039/C9NJ00061E

Moreover, the results of cytotoxicity pointed out the trend of increasing cytotoxicity (*i.e.* decreasing IC_{50} values) depending on the increasing lipophilicity of the tripodal ligands. This trend is evident either in the series of the complexes with increasing number of binuclear aryl substitution in the side-arms (quinolin-2-ylmethyl substitution) following the order of increasing lipophilicity and cztotoxicity: **1-ClO$_4$** < **4-ClO$_4$** ≈ **4-PF$_6$** < **5-ClO$_4$** ≈ **5-PF$_6$**, so in the case of the number of lipophilic substituents on pyridine rings in the following order: no substitution (**1-ClO$_4$**) < monomethyl-substitution (**2-ClO$_4$, 2-PF$_6$**) < disubstitution (dimethyl-substitution **3-PF$_6$** and dimethoxy-substitution **7-ClO$_4$**) ≈ trisubstitution (**6-ClO$_4$**, **6-PF$_6$**) < hexasubstitution (**8-ClO$_4$**).

DNA cleavage

One of the most relevant mechanisms, by which the copper(II) complexes can influence the processes of cell survival and cell death in the cancer cells, is their participation in the initiation and progression of the oxidative stress, having a strong damaging effect on various cellular targets and biomolecules.[50] The tested complexes, containing the tetradentate *N*-donor ligands, showed mild nuclease effects in the concentration-dependent manner in aqueous solutions (Fig. 2A), producing up to ca. 20 % of single-strand cleaved OC-form at the 300 μM concentration in case of **5-ClO$_4$** complex. In order to reveal whether the observed nuclease activity is based on hydrolytic or oxidative mechanism, the same experiments were performed in the absence of oxygen under inert atmosphere of helium (Fig. S1 in the ESI section). The results showed that the complexes were able to cleave the DNA in the same magnitude in the absence of oxygen (under He atmosphere) as under the normal conditions. This finding indicates that the observed small portion of DNA damage can be attributed to the direct hydrolytic mechanism.

View Article Online
DOI: 10.1039/C9NJ00061E

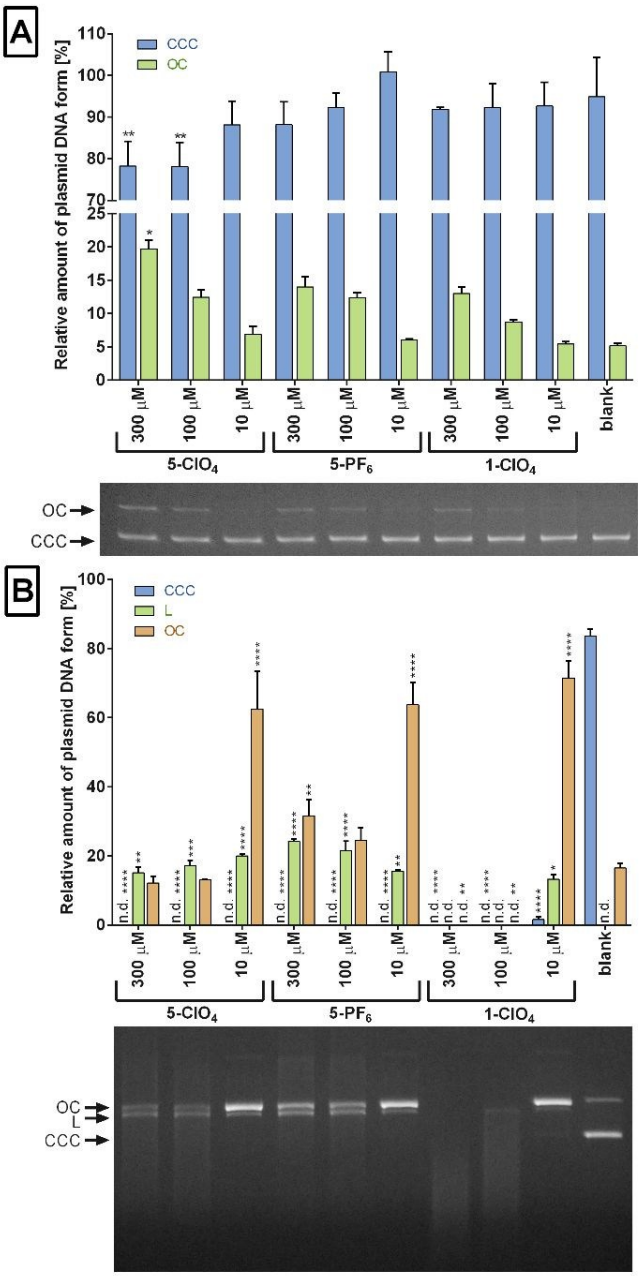

Fig. 2 Nuclease-like effect of the selected complexes (**5-ClO$_4$**, **5-PF$_6$**, **1-ClO$_4$**). Supercoiled plasmid DNA (CCC) was incubated with the complexes at different concentrations or pure solvent (blank) in the water at 37 °C for 1 h (**A**) or with the addition of 0.66 mM hydrogen peroxide (**B**). After incubation, the relative amount of open circle (OC) and linear (L) forms of plasmid DNA was evaluated by densitometric analysis. Graphs indicate means ± SEM of three independent experiments electrophoretograms show representative results of agarose electrophoresis. * indicates statistical difference to blank ($p < 0.05$); ** indicates statistical difference to blank ($p < 0.01$); **** indicates statistical difference to blank ($p < 0.0001$).

View Article Online
DOI: 10.1039/C9NJ00061E

Previous experience on this class of compounds[52,53] showed that these complexes cleave the DNA most effectively in the presence of hydrogen peroxide *via* an oxidative mechanism by taking part in the Fenton reaction.[54] In fact, dramatic increase in the nuclease activity was observed in all complexes when the reactions were performed in the presence of hydrogen peroxide (Fig. 2B). These results clearly revealed that all complexes were able not only to cleave both the single and double stranded DNA, but also were able to cleave the native CCC-form of the plasmid DNA completely even at 10 μM concentration. At higher concentrations, complete disintegration of all DNA forms to small fragments occurred (a smear was detected in the electrophoretograms) with most effective reactivity pattern determined in **1-ClO$_4$** followed by **5-ClO$_4$** and **5-PF$_6$**.

To pinpoint the participation of different reactive oxygen species (ROS) in the DNA cleavage process, the free-radical inhibitors (NaN_3, KI, and DMSO) were added into the reaction mixtures in equimolar concentrations to the applied complexes. Surprisingly, the radical scavengers produced no changes under these conditions (Figs. S2–S4). Furthermore, we checked also the effect of using high concentrations of DMSO on the cleavage process. Only when the DMSO was about 10 000-times more excess compared to the complex concentration, the cleavage process was attenuated significantly (Fig. S5). This indicates, that the hydroxyl radicals partially participate in the cleavage mechanism induced by the complexes but the major species responsible for the oxidative damage of DNA are probably metal-based intermediates which are formed in the Fenton reaction or in the mechanism of enzymatic activation of mono-copper monooxygenases such as CuO^+, CuO^+• or $[CuOOH]^+$.[54–57] This hypothesis has been indirectly confirmed by the addition of the highly efficient metal chelator EDTA to the reaction mixtures and resulted in the prevention of plasmid DNA destruction (Fig. S6).

Experimental

Materials and physical measurements

Bis(2-pyridylmethyl)amine (DPA) and 2-aminomethylpyridine as well as the hydrochloride salts of 2-chloromethylquinoline, 2-chloromethylpyridine, 3,5-dimethyl-4-methoxy-2-chloromethyl-pyridine and 3,4-dimethoxy-2-chloromethylpyridine were purchased from TCI-America, whereas 6-methyl-2-pyridinemethanol was purchased from Alfaaesar. All other chemicals were commercially available and used without further purification. Infrared spectra were recorded on a JASCO FTIR-480 plus spectrometer as KBr pellets or on a Cary 630 (ATR-IR) spectrometer. Electronic spectra were

View Article Online
DOI: 10.1039/C9NJ00061E

recorded using an Agilent 8453 HP diode array UV-Vis spectrophotometer. ^{1}H and ^{13}C NMR spectra were obtained at room temperature on a Varian 400 NMR spectrometer operating at 400 MHz (^{1}H) and 100 MHz (^{13}C). ^{1}H and ^{13}C NMR chemical shifts (δ) are reported in ppm and were referenced internally to residual solvent resonances (DMSO-d_6: δ_H = 2.49, δ_C = 39.4 ppm). ESI-MS were measured on Agilent 6210 electrospray TOF mass spectrometer. The conductivity measurements were performed using Mettler Toledo Seven Easy conductivity meter and calibrated by the aid of 1413 μS/cm conductivity standard. The molar conductivities of the complexes were determined from Λ_M = (1.0 x10^3 κ)/[Cu], where κ = specific conductance and [Cu] is the molar concentration of the complex. Elemental microanalyses were carried out by Atlantic Microlaboratory, Norcross, Georgia U.S.A.

***Caution**: Salts of perchlorate and their metal complexes are potentially explosive and should be handled with great care and in small quantities.*

Synthesis of the ligands

Tris(2-pyridymethyl)amine (TPA), [(6-methyl-2-pyridyl)methyl)-bis(2-pyridylmethyl)]amine (6-MeTPA), [bis(6-methyl-2-pyridyl)methyl)-(2-pyridylmethyl)]amine (6-Me_2TPA), [bis(2-pyridylmethyl)-(2-quinolylmethyl)]amine (BPQA), [bis(2-quinolylmethyl)-(2-pyridylmethyl)]amine (BQPA), [(3,5-dimethyl-4-methoxy-2-pyridylmethyl)-bis(2-pyridylmethyl)]amine (L^1), [(3,4-dimethoxy-2-pyridylmethyl)-bis(2-pyridylmethyl)]amine (L^2) and [bis(3,5-dimethyl-4-methoxy-2-pyridylmethyl)-(2-pyridylmethyl)]amine (L^3) were synthesized according to the published procedure [39,40]. The conversion of 6-methyl-2-pyridinemethanol into 6-methyl-2-chloromethylpyridine hydrochloride was achieved in CCl_4 by $SOCl_2$, followed by recrystallization from ethanol.

Synthesis of the complexes

The complex **[Cu(TPA)Cl]ClO_4·½H_2O** (**1-ClO_4**) was synthesized as described.[41]

[Cu(6-MeTPA)Cl]ClO_4 (2-ClO_4). Although this complex was previously synthesized and structurally characterized,[43] here in we described its synthesis which is slightly modified from the reported one. A mixture containing [(6-methyl-2-pyridyl)-methyl)-bis(2-pyridylmethyl)]amine (6-MeTPA), (0.152 g, 0.50 mmol) and $CuCl_2·2H_2O$ (0.090 g, 0.5 mmol) dissolved in MeOH (20 mL) was heated on a steam-bath for 5 min. To this solution $NaClO_4$ (0.070 g, 0.57 mmol) was followed by

View Article Online
DOI: 10.1039/C9NJ00061E

filtration through celite. The resulting solution was allowed to stand at room temperature. After one day, the blue precipitate, which separated was collected by filtration, recrystallized from CH_3CN to remove unreacted $NaClO_4$ and allowed to evaporate at room temperature. The resulting blue precipitate was collected and further recrystallization of the product from MeOH afforded good single crystals suitable for X-ray analysis. These were washed with propan-2-ol and Et_2O, and dried in air (yield: 0.210 g, 84%). Characterization: *Anal*. Calcd for $C_{19}H_{20}CuCl_2N_4O_4$ (502.84 g/mol): C, 45.38; H, 4.01; N, 11.14. Found: C, 45.39; H, 4.06; N, 11.10%. ESI-MS (CH_3CN): *m/z* = 402.07 (Calcd for $[C_{19}H_{20}ClCuN_4]^+$ = 402.08, 100%) and 98.95 (Calcd for ClO_4^- = 98.95, 100%). Selected IR bands (ATR-IR, cm^{-1}): 1604 (s), 1438 (s), 1372 (w), 1261 (w), 1167 (w), 1078 (vs), 1023 (vs), 1007 (w), 955 (m), 768 (m). UV-Vis (CH_3CN), λ_{max}, nm (ε_{max}, cm^{-1} M^{-1}): ~660 (sh), 900 (112, b). Λ_M (CH_3CN) = 142 $\Omega^{-1}cm^2mol^{-1}$.

[Cu(6-Me$_2$TPA)Cl]PF$_6$ (3-PF$_6$). To a mixture containing [bis(6-methyl-2-pyridyl)methyl)-(2-pyridylmethyl)]amine (6-Me$_2$TPA) (0.152 g, 0.50 mmol) and $CuCl_2 \cdot 2H_2O$ (0.090 g, 0.5mmol) dissolved in MeOH (20 mL) NH_4PF_6 (0.098 g, 0.60 mmol) was added. The bluish-torques solution was heated on a steam-bath for 5 min, filtered through celite and then was allowed to stand at room temperature. The crude product which separated after one day was collected by filtration, recrystallized from CH_3CN to remove unreacted NH_4PF_6 and allowed to evaporate at room temperature. Recrystallization from MeOH afforded good blue single crystals suitable for X-ray analysis. These were collected by filtration, washed with propan-2-ol and Et_2O, and dried in air (yield: 0.240 g, 85%). Characterization: *Anal*. Calcd for $C_{20}H_{22}ClCuF_6N_4P$ (562.38 g/mol): C, 42.71; H, 3.94; N, 9.96. Found: C, 42.61; H, 3.97; N, 9.86%. Selected IR bands (ATR-IR, cm^{-1}): 3100 (vw), 2954 (vw), 1600 (m), 1574 (w), 1467 (w), 1443 (m), 1284 (m), 1167 (m), 1092 (m), 1007 (m), 970 (w), 827 (vs). UV-Vis (CH_3CN), λ_{max}, nm (ε_{max}, cm^{-1} M^{-1}): 685 (148), ~860 (sh). Λ_M (CH_3CN) = 146 $\Omega^{-1}cm^2mol^{-1}$.

The rest of the complexes were typically synthesized using the appropriate ligand and a procedure similar to that described either for the perchlorate complex, [Cu(6-MeTPA)Cl]ClO_4 (**2-ClO$_4$**)[43] or the hexafluorophosphate, [Cu(6-Me$_2$TPA)Cl]PF_6 (**3-PF$_6$**).

[Cu(6-MeTPA)Cl]PF$_6$ (2-PF$_6$). Blue crystals were obtained from a green solution (yield: 0.200 g, 73%). Characterization: *Anal*. Calcd. for $C_{19}H_{20}ClCuF_6N_4P$ (548.35 g/mol): C, 41.62; H, 3.68;

View Article Online
DOI: 10.1039/C9NJ00061E

N, 10.22. Found: C, 41.68; H, 3.80; N, 10.17%. ESI-MS (CH_3CN): *m/z* = 402.07 (Calcd for $[C_{19}H_{20}ClCuN_4]^+$ = 402.08, 100%) and 144.97 (Calcd for PF_6^- = 144.96, 100%). Selected IR bands (ATR-IR, cm^{-1}): 1611 (s), 1576 (m), 1482 (m), 1459 (m), 1446 (s), 1161 (m), 1105 (m), 1056 (m), 1031 (m), 840 (vs), 770 (w). UV-Vis (CH_3CN), λ_{max}, nm (ε_{max}, cm^{-1} M^{-1}): ~670 (sh), 885 (132, b). Λ_M (CH_3CN) = 143 $\Omega^{-1}cm^2mol^{-1}$.

[Cu(BPQA)Cl]ClO_4 (4-ClO_4). Blue crystalline compound (yield: 0.180 g, 67%). Characterization: *Anal*. Calcd for $C_{22}H_{20}Cl_2CuN_4O_4$ (538.87 g/mol): C, 49.03; H, 3.74; N, 10.40. Found: C, 49.08; H, 3.90; N, 10.29%. Selected IR bands (ATR-IR, cm^{-1}): 3060 (w), 2965 (vw), 1600 (s), 1571 (m), 1507 (m) 1472 (m), 1433 (s), 1284 (m), 1156 (m), 1078 (vs), 906 (m), 833 (s), 779 (s), 768 (s), 728 (m). UV-Vis (CH_3CN), λ_{max}, nm (ε_{max}, cm^{-1} M^{-1}): ~640, 880 (151, b). Λ_M (CH_3CN) = 141 $\Omega^{-1}cm^2mol^{-1}$.

[Cu(BPQA)Cl]PF_6 (4-PF_6). Long green needles (yield: 0.210 g, 72%). Characterization: *Anal*. Calcd. for $C_{22}H_{20}ClCuF_6N_4P$ (584.38 g/mol): C, 45.22; H, 3.45; N, 9.59. Found: C, 45.55; H, 3.36; N, 9.59%. Selected IR bands (ATR-IR, cm^{-1}): 3080 vw), 3063 (vw), 2968 (vw), 2923 (vw), 1610 (s), 1599 (m), 1509 (w), 1482 (w), 1446 (m), 1286 (m), 1158 (m), 1102 (w), 1054 (m), 1030 (w), 964 (m), 891 (m), 830 (vs), 769 (s). UV-Vis (CH_3CN), λ_{max}, nm (ε_{max}, cm^{-1} M^{-1}): ~700 (sh), 900 (159, b). Λ_M (CH_3CN) = 147 $\Omega^{-1}cm^2mol^{-1}$.

[Cu(BQPA)Cl]ClO_4 (5-ClO_4). Blue crystalline compound (yield: 0.24 g, 75%). Characterization: *Anal*. Calcd for $C_{26}H_{22}Cl_2CuN_4O_4$ (588.93 g/mol): C, 53.02; H, 3.77; N, 9.51. Found: C, 52.93; H, 3.63; N, 9.41%. Selected IR bands (ATR-IR, cm^{-1}): 3072 (w), 2932 (vw), 1600 (s), 1570 (m), 1513 (s), 1474 (m), 1434 (m), 1370 (w), 1344 (w), 1299 (m), 1208 (m), 1074 (vs), 1017 (s), 955 (s), 908 (w), 838 (s), 829 (s), 780 (vs), 761 (s), 748 (m). UV-Vis (CH_3CN) λ_{max}, nm (ε_{max}, cm^{-1} M^{-1}): 730 (138, b), ~880 (143, b). Λ_M (CH_3CN) = 145 $\Omega^{-1}cm^2mol^{-1}$.

[Cu(BQPA)Cl]PF_6 (5-PF_6). Olive green crystalline compound (yield: 0.220 g, 69%). Characterization: *Anal*. Calcd for $C_{26}H_{22}Cl_2CuN_4O_4$ (634.44 g/mol): C, 49.22; H, 3.50; N, 8.83. Found: C, 49.56; H, 3.53; N, 8.96%. Selected IR bands (ATR-IR, cm^{-1}): 3072 (w), 2934 (vw), 2871 (vw), 1601 (s), 1571 (m), 1515 (m), 1470 (m), 1446 (s), 1374 (m), 1312 (m), 1209 (m), 1022 (m), 967 (m), 847 (vs), 779 (s), 558 (s). UV-Vis (CH_3CN), λ_{max}, nm (ε_{max}, cm^{-1} M^{-1}): ~660 (sh), 880 (141, b). Λ_M (CH_3CN) = 146 $\Omega^{-1}cm^2mol^{-1}$.

View Article Online
DOI: 10.1039/C9NJ00061E

[Cu(L^1)Cl]ClO$_4$ (6-ClO$_4$). Green crystalline compound (yield: 0.160 g, 59%). Characterization: *Anal*. Calcd for $C_{21}H_{24}Cl_2CuN_4O_5$ (546.89 g/mol): C, 46.12; H, 4.42; N, 10.24. Found: C, 45.93; H, 4.53; N, 10.41%. ESI-MS (CH_3CN): *m/z* = 446.09 (Calcd for $[C_{21}H_{24}ClCuN_4O]^+$ = 446.10, 100%), 411.12 (Calcd for $C_{21}H_{24}CuN_4O$ = 411.13), 98.95 (Calcd for ClO_4^- = 98.95, 100%). Selected IR bands (ATR-IR, cm^{-1}): 3068 (vw), 3027 (vw), 2942 (w), 1607 (s), 1478 (s), 1445 (s), 1405 (m), 1267 (s), 1093 (vs), 957 (w), 878 (w), 768 (s). UV-Vis (CH_3CN), λ_{max}, nm (ε_{max}, cm^{-1} M^{-1}): ~725 (sh), 955 (221). Λ_M (CH_3CN) = 143 Ω^{-1}cm^{2}mol^{-1}.

[Cu(L^1)Cl]PF$_6$ (6-PF$_6$). Green crystalline compound (yield: 0.150 g, 51%). Characterization: *Anal*. Calcd for $C_{21}H_{24}ClCuF_6N_4OP$ (592.41 g/mol): C, 42.58; H, 4.08; N, 9.46. Found: C, 42.52; H, 4.02; N, 9.37%. Selected IR bands (ATR-IR, cm^{-1}): 3103 (vw), 3089 (vw), 3030 (vw), 1607 (s), 1576 (m), 1479 (s), 1445 (s), 1267 (s), 1081 (s), 1023 (m), 996 (m), 958 (m), 835 (vs), 557 (s). UV-Vis (CH_3CN), λ_{max}, nm (ε_{max}, cm^{-1} M^{-1}): ~700 (sh), ~ 850 (sh), 970 (355). Λ_M (CH_3CN) = 147 Ω^{-1}cm^{2}mol^{-1}.

[Cu(L^2)Cl]ClO$_4$ (7-ClO$_4$). Green crystalline compound (yield: 0.170 g, 62%). Characterization: *Anal*. Calcd for $C_{20}H_{22}Cl_2CuN_4O_6$ (548.86 g/mol): C, 43.77; H, 4.04; N, 10.21. Found: C, 43.57; H, 4.11; N, 10.15%. Selected IR bands (ATR-IR, cm^{-1}): 3105 (vw), 3064 (vw), 2926 (w), 2854 (vw), 1604 (s), 1498 (s), 1442 (m), 1305 (s), 2060 (vs), 1451 (m), 1393 (m), 1092 (vs), 1063 (vs), 1007 (w), 845 (m), 772 (m). UV-Vis (CH_3CN), λ_{max}, nm (ε_{max}, cm^{-1} M^{-1}): ~715 (sh), 960 (230, b). Λ_M (CH_3CN) = 149 Ω^{-1}cm^{2}mol^{-1}.

[Cu(L^3)Cl]ClO$_4$ (8-ClO$_4$). Aquamarine crystalline compound (yield: 0.280 g, 93%) was obtained upon recrystallization from CH_3CN. Characterization: *Anal*. Calcd for $C_{24}H_{30}Cl_2CuN_4O_6$ (604.97 g/mol): C, 47.65; H, 5.00; N, 9.26. Found: C, 47.37; H, 4.93; N, 9.22%. ESI-MS (CH_3CN): *m/z* = 504.13 (Calcd for $[C_{24}H_{30}ClCuN_4O_2]^+$ = 504.15, 100%), 469.17 (Calcd for $C_{24}H_{30}CuN_4O_2$ = 469.18), 98.95 (Calcd for ClO_4^- = 98.95, 100%). Selected IR bands (ATR-IR, cm^{-1}): 3166 (vw), 3132 (vw), 2926 (w), 2860 (w), 1552 (m), 1470 (m), 1419 (m), 1272 (m), 1143 (s), 1114 (vs), 1090 (vs). UV-Vis (CH_3CN), λ_{max}, nm (ε_{max}, cm^{-1} M^{-1}): ~710 (sh), ~880 (sh), 970 (371). Λ_M (CH_3CN) = 137 Ω^{-1}cm^{2}mol^{-1}.

X-Ray crystallography

View Article Online
DOI: 10.1039/C9NJ00061E

The X-ray single-crystal data of compounds were collected on a Bruker-AXS APEX-II CCD diffractometer at 100(2) K. The crystallographic data, conditions retained for the intensity data collection and some features of the structure refinements are listed in Table 4. The intensities were collected with Mo-Kα radiation (λ= 0.71073 Å). Data processing, Lorentz-polarization and absorption corrections were performed using SAINT, APEX and the SADABS computer programs.[58,59] The structures were solved by direct methods and refined by full-matrix least-squares methods on F^2, using the SHELX program package.[60,61] All non-hydrogen atoms were refined anisotropically. The hydrogen atoms were located from difference Fourier maps, assigned with isotropic displacement factors and included in the final refinement cycles by use of geometrical constraints. Complex **6-PF$_6$** was refined as a 2-component inversion twin. Molecular plots were performed with the Mercury program.[62]

View Article Online
DOI: 10.1039/C9NJ00061E

Table 4 Crystallographic data and processing parameters

Compound	**2-PF_6**	**4-ClO_4**	**4-PF_6**	**5-PF_6**
Empirical formula	$C_{19}H_{20}ClCuF_6N_4P$	$C_{22}H_{20}Cl_2CuN_4O_4$	$C_{22}H_{20}ClCuF_6N_4P$	$C_{26}H_{22}ClCuF_6N_4P$
Formula mass	548.36	538.87	584.39	634.45
System	Monoclinic	Monoclinic	Monoclinic	Monoclinic
Space group	$P2_1/c$	$P2_1/n$	$P2_1/n$	C2/c
a (Å)	11.8757(5)	12.3694(5)	12.7761(4)	33.4625(10)
b (Å)	13.1776(6)	12.6452(5)	12.9219(4)	9.7014(3)
c (Å)	15.2002(6)	14.7677(6)	14.6930(5)	15.7910(5)
α (°)	90	90	90	90
β (°)	112.138(2)	106.807(2)	106.900(2)	91.518(1)
γ (°)	90	90	90	90
V ($Å^3$)	2203.37(16)	2211.20(16)	2320.93(13)	5124.5(3)
Z	4	4	4	8
T (K)	100(2)	100(2)	100(2)	100(2)
μ (mm^{-1})	1.250	1.268	1.193	1.088
D_{calc} (Mg/m^3)	1.653	1.619	1.673	1.645
Crystal size (mm)	0.22 x 0.19 x 0.14	0.29 x 0.24 x 0.13	0.18 x 0.17 x 0.08	0.25 x 0.21 x 0.14
θ max (°)	30.104	30.082	27.996	29.998
Data collected	77316	103512	49562	137606
Unique refl. / R_{int}	6437 / 0.0611	6468 / 0.0603	5588 / 0.0340	7473 / 0.0351
Parameters / Restraints	290 / 0	344 / 25	353 / 0	352 / 0
Goodness-of-Fit on F^2	1.006	1.068	1.017	1.019
R1 / wR2 (all data)	0.0362 / 0.0921	0.0287 / 0.0660	0.0240 / 0.0681	0.0228 / 0.0644
Residual extrema ($e/Å^3$)	1.09 / -0.63	0.44 / -0.43	0.38 / -0.30	0.50 / -0.37

View Article Online
DOI: 10.1039/C9NJ00061E

Table 4 Crystallographic data and processing parameters

Compound	**7-ClO_4**	**8-ClO_4**	**6-PF_6**
Empirical formula	$C_{20}H_{22}Cl_2CuN_4O_6$	$C_{24}H_{30}Cl_2CuN_4O_6$	$C_{21}H_{24}ClCuF_6N_4OP$
Formula mass	548.87	604.98	592.41
System	Orthorhombic	Monoclinic	Triclinic
Space group	$P2_12_12_1$	$P2_1/c$	P-1
a (Å)	9.2019(5)	16.9159(6)	14.5459(10)
b (Å)	11.2119(6)	8.7895(3)	18.4758(12)
c (Å)	21.9518(11)	19.0235(7)	18.4808(3)
α (°)	90	90	97.653(3)
β (°)	90	112.756(2)	93.831(3)
γ (°)	90	90	93.870(3)
V ($Å^3$)	2264.8(2)	2608.29(16)	4896.8(6)
Z	4	4	8
T (K)	100(2)	100(2)	100(2)
μ (mm^{-1})	1.246	1.089	1.135
D_{calc} (Mg/m^3)	1.610	1.541	1.607
Crystal size (mm)	0.17 x 0.16 x 0.09	0.26 x 0.20 x 0.15	0.14 x 0.11 x 0.08
θ max (°)	30.089	29.998	27.000
Data collected	55536	132850	305982
Unique refl. / R_{int}	6635 / 0.0559	7607 / 0.0718	21360 / 0.0990
Parameters / Restraints	346 / 48	340 / 0	1262 / 12
Goodness-of-Fit on F^2	1.018	1.010	1.042
R1 / wR2 (all data)	0.0219 / 0.0537	0.0301 / 0.0766	0.0648 / 0.1852
Residual extrema ($e/Å^3$)	0.31 / -0.24	0.54 / -0.52	1.42 / -0.99

CCDC 1885301-1885307 contain the crystallographic data in CIF format for **2-PF_6**, **4-ClO_4**, **4-PF_6**, **5-PF_6**, **7-ClO_4**, **8-ClO_4** and **6-PF_6**, respectively.

MTT Cell viability assay

The human cancer cell lines A2780, A2780R and MCF7 were obtained from ECACC and cultivated according to the producer's protocols. The cells were treated with the tested compounds and a

View Article Online
DOI: 10.1039/C9NJ00061E

reference drug *cisplatin* in the concentrations up to 100 μM for 24 h, using the 96-well culture plates. In parallel, the cells were treated with the vehicle (0.1% v/v DMF) and Triton X-100 (1%, v/v) to assess the minimal, and maximal cell damage, respectively. MTT assay was performed and absorbance was measured spectrophotometrically at 570 nm on an Infinite M200 (Schoeller Instruments, Prague, Czech Republic). The data were expressed as the percentage of cell viability, where 100% and 0% represent the treatments with the negative control (DMF), and positive control (Triton X-100), respectively. Half-maximal inhibitory concentrations (IC_{50}) were calculated using GraphPad Prism 6 software (GraphPad Software, San Diego, USA).

DNA cleavage studies

Isolation of plasmid DNA

The ability of metal complexes to act as chemical nucleases was evaluated using the pUC19 plasmid (2686 bp). Plasmids were isolated from the transformed bacteria *Escherichia coli* TOP10F' by the QIAprep Spin Miniprep Kit (Qiagen, Hilden, Germany) according to the manufacturer`s instruction. Plasmid DNA was eluted from the column by nuclease-free ultrapure water and it was used in the DNA cleavage assays within 96 h after isolation. The quantity and purity of isolated DNA was measured spectrophotometrically at 230, 260, 280, and 320 nm. The absorbance ratio A_{260}/A_{280} was in the range between 1.75 and 1.85, and the absorbance ratio A_{260}/A_{230} was in the range between 2.00 and 3.00 which confirmed that the DNA was free of proteins, RNA and other impurities.

Interactions of the complexes with the plasmid DNA

The nuclease activity of the two most cytotoxic complexes **5-ClO$_4$** and **5-PF$_6$** as well as the less active complex **1-ClO$_4$** was determined using the previously published method with small modifications.[52] The 300 ng of the native supercoiled pUC19 plasmid DNA (*i.e.* 23.1 μM of base pairs in the final

View Article Online
DOI: 10.1039/C9NJ00061E

volume of 20 µL of reaction mixture) was incubated either in the presence or in the absence of 0.66 mM hydrogen peroxide, and together with different concentrations of the tested complexes dissolved in acetonitrile (at the concentration levels of 0, 10, 100, and 300 µM, while the final concentration of acetonitrile was 10 % (v/v) in the reaction mixture) at 37° C for 1 h. Immediately after this, the samples were thoroughly mixed with 6X gel loading buffer (containing 60 mM EDTA, 60% (v/v) glycerol and 0.03% (w/v) bromphenol blue) and subsequently loaded on a 0.8% (w/v) agarose gel prepared in TBE buffer (containing 89 mM Tris-borate buffer and 2 mM EDTA; Sigma-Aldrich) impregnated with 0.15 µg/mL of ethidium bromide (EtBr). The electrophoreograms were analysed by the AlphaEaseFC version 4.0.0.34 software (Alpha Innotech, USA) and the relative amounts of the supercoiled circular (CCC-form), single-strand nicked (OC-form) and linear (L-form) forms were evaluated. The quantification of CCC-form of plasmid DNA was corrected by a factor of 1.47.[39] The relative amount of each plasmid form was calculated as a percentage of total amounts of DNA in the negative control containing the native form of plasmid DNA only. To clarify if the DNA cleavage is caused by oxidative or hydrolytic mechanisms, the reactions of complexes and plasmid DNA in aqueous solutions were performed under the inert atmosphere (solutions were bubbled with helium before use). The other reaction conditions remained unchanged (see above).

Effect of the antioxidants and other inhibitors on the plasmid DNA cleavage

To understand the role of reactive oxygen species or other mechanisms in the DNA cleavage process, the reaction mixtures were also supplemented with the various ROS scavengers, specifically NaN_3 (a selective quencher of reactive singlet oxygen),[63] DMSO and KI (very effective scavengers for hydroxyl radicals),[64] and highly efficient EDTA metal chelator. All antioxidants and inhibitors, except DMSO, were added to the reaction mixtures in the molar ratio of 1:1 with 300 µM and 10 µM concentrations of the complexes and these were incubated with the plasmid DNA in a similar manner

View Article Online
DOI: 10.1039/C9NJ00061E

as that described above. In the case of DMSO, molar ratios 1:100 and 1:10 000 were also used instead. After densitometric analysis of the obtained electrophoreograms, the relative amount of each plasmid form was calculated as a percentage of total amounts of DNA.

Statistical evaluation

All experiments were performed at least in three independent repetitions. The statistical analysis of the obtained data was performed using the GraphPad Prism 6.01 software (GraphPad Software, Inc., La Jolla, CA, USA) and ANOVA test with multiple comparisons followed by Bonferroni *post-hoc* test was applied.

Conclusions

A series of five-coordinate chlorido-Cu(II) complexes has been synthesezed, using tetradentate *N*-donor tripod pyridyl amine derivatives, and structurally characterized: $[Cu(TPA)Cl]ClO_4.½H_2O$ (**1-ClO$_4$**), $[Cu(6\text{-}MeTPA)Cl]ClO_4/PF_6$ (**2-ClO$_4$/2-PF$_6$**), $[Cu(6\text{-}Me_2TPA)Cl]PF_6$ (**3-PF$_6$**), $[Cu(BPQA)Cl]ClO_4/PF_6$ (**4-ClO4/4-PF$_6$**), $[Cu(BPQA)Cl]ClO_4/PF_6$ (**4-ClO$_4$/4-PF$_6$**), $[Cu(BQPA)Cl]ClO_4/PF_6$ (**5-ClO$_4$/PF$_6$**), $[Cu(L^1)Cl]ClO_4/PF_6$ (**6-ClO$_4$/6-PF$_6$**), $[Cu(L^2)Cl]ClO_4$ (**7-ClO$_4$**) and $[Cu(L^3)Cl]ClO_4$ (**8-ClO$_4$**). In acetonitrile or aqueous acetonitrile solution, all the complexes display TBP with the exception of **3-PF$_6$** which exhibits SP and **5-ClO$_4$** which has an intermediate geometry. The *in vitro* cytotoxicity studies of the complexes against A2780 (ovarian), A2780R (cisplatin-resistant variant) and MCF7 (breast cancer) human cancer cell lines revealed moderate-to-significant effects compared to the reference *cisplatin* drug. Interestingly, **5-ClO$_4$** and **5-PF$_6$** compounds showed very high anticancer activities in the three tested cancer cell lines, with the best IC_{50} values about 8–10 μM). The DNA cleavage studies demonstrated that the studied complexes are effective in causing the DNA damage by means of the minor direct hydrolytic cleavage and major oxidative mechanism

View Article Online
DOI: 10.1039/C9NJ00061E

(associated probably with the formation of oxidative metal-based intermediates, similar to those formed in the enzymatic mechanism of mono-copper monooxygenases, such as CuO^+, CuO^+• or $[CuOOH]^+$).

Abbreviations. TPA = tris(2-pyridylmethyl)amine, 6-MeTPA = [(6-Methyl-2-pyridyl)methyl)bis(2-pyridylmethyl)]amine, 6-Me_2TPA = [bis(6-Methyl-2-pyridyl)methyl)-(2-pyridylmethyl)]amine, BPQA = [bis(2-pyridylmethyl)-(2-quinolylmethyl)]amine, BQPA = [bis(2-quinolylmethyl)-(2-pyridylmethyl)]amine, L^1 = [(3,5-dimethyl-4-methoxy-2-pyridylmethyl)-bis(2-pyridylmethyl)]amine, L^2 = [(3,4-dimethoxy-2-pyridylmethyl)-bis(2-pyridylmethyl)]amine, L^3 = [bis(3,5-dimethyl-4-methoxy-2-pyridylmethyl)-(2-pyridylmethyl)]amine, MTT = 3-(4,5-dimethylthiazol-2-yl)-2,5-diphenyltetrazolium bromide, A2780: ovarian cancer, A2780R: cisplatin-resistant variant, MCF7: breast cancer cell line

Acknowledgments This research was financially supported by the Department of Chemistry-UL Lafayette. FAM thanks Dr. J. Baumgartner (TU Graz) for assistance and NAWI Graz for support. JV, JH, ZD and ZT acknowledge the financial support from Ministry of Education, Youth and Sports of the Czech Republic, NPU I (a grant no. LO1305).

References

1. N. Howlader, M. Krapcho, J. Carshell, N. Neyman, S. F. Alterkruse, C. L. Kosary, M. Yu, J. Ruhl, Z. Zatalovich, H. Cho, A. Mariotto, D. R. Lewis, H. S. Chen, E. J. Feuer and K. A. Cronin (eds), April 2013, pp. N. Howlader, A. M. Noone, M. Krapcho, J. Carshell, N. Neyman, S. F. Alterkruse, C. L. Kosary, M. Yu, J. Ruhl, Z. Zatalovich, H. Cho, A. Mariotto, R. Lewis, H. S. Chen and E. J. Feuer (Eds), SEER Cancer Statistics Review, 1975-2010, National Cancer Institute, Bethesda, MD (http://seer.cancer.gov/csr/1975-2010/, based on November 2012 SEER data submission, posted to the SEER web site, April 2013).
2. J. Ferlay, H. R. Shin, F. Bray, D. Forman, C. Mathers and D. M. Parkin, *GLOBCAN*, 2010, 2008 v2.0, Cancer Incidence and Mortality Worldwide: IARC Cancer Base No. 10, Lyon, France: International Agency for Research on Cancer, (http://globocan.iarc.fr, 06/06/2016).
3. T. C. Johnstone, K. Suntharalingam and S. J. Lippard, *Chem. Rev.*, 2016, **116**, 3436–3486.
4. T. Boulikas and M. Vougiouka, *Oncology Reports*, 2003, **10**, 1663-1682.

View Article Online
DOI: 10.1039/C9NJ00061E

5. L. R. Kelland, *Drugs*, 2000, 591-598.

6. C. Marzano, M. Pellei, F. Tisato and C. Santini, *Med. Chem.*, 2009, 9185-9211.

7. I. Ott and R. Gust, *Arch. Pharm. Chem. Life SC*, 2007, **340**, 117-126.

8. O. Dömötör, R. F. M. de Almeida, L. Côrte-Real, C. P. Matos, F. Marques, A. Matos, C. Real, T. Kiss, E. A. Enyedy, M. H. Garcia and A. I. Tomaz, *J. Inorg. Biochem.*, 2017, **168**, 27-37.

9. A. Bergamo and G. Sava, *Dalton Trans.*, 2007, 1267-1272.

10. M. J. Clarke, *Coord. Chem. Rev.*, 2003, **236**,209-233.

11. C. R. Munteanu and K. Suntharalingam, *Dalton Trans.*, 2015, **44**, 13796-13808.

12. R. Tabti, N. Tounsi, C. Gaiddon, E. Bentouhami and L. Désaubry, *Med. Chem. (Los Angleos)*, 2017, **7**, 875-879.

13. C. Santini, M. Pellei, V. Gandin, M. Porchia and F. Tisato, *Chem. Rev.*, 2014, **144**, 815-862.

14. E. Ramachandran, V. Gandin, R. Bertani, P. Sgarbossa, K. N. Nattamai, S. P. Bhuvanesh, A. Venzo, A. Zoleo, A. Glisenti, A. Dolmella, A. Albinati and C. J. Marzano, *Inorg. Biochem.*, 2018, **182**,18-28.

15. J. Hu, C. Liao, R. Mao, J. Zhang, J. Zhao and Z. Gu, *Med. Chem. Commun.*, 2018, **9**, 337-343.

16. A. M. Gouda, H. A. El-Ghamry, T. M. Bawazeer, T. A. Farghaly, A. N. Abdallagh and A. Aslami, *Eur. J. Med. Chem.*, 2018, **145**, 350-359

17. K. Hu, F. Li, Z. Feiyan, Z. Zhang and F. Liang, *New J. Chem.*, 2017, **41**,2062-2072.

18. W. Villarreal, L. Colina-Vegas, C. Visbal, O. Corona, R. S. Corrêa, J. Ellena, M. R. Cominetti, A. A. Batista and M. Navarro, *Inorg. Chem.*, 2017, **56**, 3781-3793.

19. B. Deka, T. Sarkar, S. Banerjee, A. Kumar, S. Mukherjee, S. Deka, K. K. Sailkia and A. Hussain, *Dalton Trans.*, 2017, **46**, 396-409.

20. D. Montagner, B. Fresch, K. Browne, V. Gandian and A. Erxleben, *Chem. Comm.*, 2017, **53**, 134-137.

21. N. R. Angel, R. M. Khatib, J. Jenkins, M. Smith, J. M. Rubalcava, B. K. Le Daniel Lussier, Z. Chen, F. S. Tham, E. H. Wilson and J. F. Eichler, *J. Inorg. Biochem.*, 2017, **166**, 12-25.

22. C. Acilan, B. Cevatemre Z. Adiguzel, D. Karakas, E. Ulukaya, N. Riberio, I. Correia and J. C. Pessoa, *Biochimmica et Biophysica Acta*, 2017, **1861**, 218-234

23. C. Marzano, M. Pellei, F. Tisato and C. Santini, *Anti-Cancer Agents in Medicinal Chemistry* 2009, **9**, 185-211

View Article Online
DOI: 10.1039/C9NJ00061E

24. C. C. Bavisotto, N. Nikolic, A. M. Gammaza, R. Barone, F. L. Cascio, E. Mocciaro, G. Zummo, E. C. de Macairo, A. J. Macario, F. Cappelo, V. Giacalone, A. Pace, G. Barone, A. B. Piccionello and G. Campanella, *J. Inorg. Biochem.*, 2017, **170**, 8-16.

25. L. M. López-Martinez, H. Santacruz-Ortega, R. E. Navarro, M. Inoue, R. Sugich-Miranda, J. Hernández-Paredes, I. Castillo and R. R. Sotelo-Mundo, *Polyhedron*, 2017, **127**, 438-448.

26 M. Jopp, J. Becker, S. Becker, M. Miska, V. Gandin, C. Marzano and S. Schindler, *Eur. J. Med. Chem.*, 2017, **132**, 274-281.

27. S. M. G. Leite, L. M. P. Lima, S. Gama, F. Mendes, M. Orio, S. Bento, A. Paulo, R. Delgado and O. Iranzo, *Inorg. Chem*., 2016, **55**, 11801-11814.

28. Y. Du, W. Chen, X. Fu, H. Deng and J.-G. Deng, *RSC Adv.*, 2016, **6**, 109718-109725.

29. F. N. Akladios, S. D. Andrew and C. J. Parkinson, *J. Biol. Inorg. Chem.*, 2016, **21**, 931-944.

30. U. K. Komarnicka, R. Starosta, A. Kyzioł, M. Płotek, M. Puchalska and M. Jeżowska-Bojczuk, *J. Inorg. Biochem.*, 2016, **165**, 25-35.

31. S. S. Massoud, F. R. Louka G. T. Ducharme, R. C. Fischer, F. A. Mautner, J. Vančo, R. Herchel, Z. Dvořák and Z. Trávníček, *J. Inorg. Biochem.*, 2018, **180**, 39-46.

32. R. Herchel, Z. Dvořák, Z. Trávníček, M. Mikuriya, F. R. Louka, F. A. Mautner and S. S. Massoud, *Inorg. Chim. Acta*, **2016**, 451,102-110.

33. W. M. T. Q. de Medeiros, M. J. C. de Medeiros, E. C. Carvalho, J. A. de Lima, V. da S. Oliveira, A. C. de B Pontes, F. O. N. da Silva, J. A. Ellena, H. A. de O Rocha, E. H. S. de Sousa and de D. L. Pontes, *RSC Adv.*, 2018, **8**, 16873-16886.

34. D. Mahendiran, S. Amuthakala, N. S. P. Bhuvanesh, R. S. Kumarc and A. K. Rahiman, *RSC Adv.*, 2018, **8**, 16973-16990.

35. C. Slator, Z. Molphy, V. McKee, C. Long, T. Brown and A. Kellett, *Nucleic Acids Research*, 2018, **46**, 2733–2750.

36. J. C. Dabrowiak, Metals in Medicine, John Wiley & Sons. Ltd, West Sussex, U.K. 2009, pp. 235-238.

37. Z. Tyeklár, R. R. Jacobson, N. Wei, N. N. Murthy, J. Zubieta and K. D. Karlin, *J. Am. Chem. Soc.*, 1993, **115**, 2677-2689.

38. U. Mukhopadhyay, I. Bernal, S. S. Massoud and F. A. Mautner, *Inorg. Chim. Acta*, 2004, **357**, 3673-2682.

39. S. S. Massoud, R. S. Perkins, F. R. Louka, W. Xu, A. Le Roux, Q. Dutercq, R. C. Fischer, F. A. Mautner, M. Handa, Y. Hiraoka, G. L. Kreft, T. Bortolotto and H. Terenzi, *Dalton Trans.*, 2014, **43**, 10086-10103.

40. S. D. Kettenmann, F. R. Louka, E. Marine, R. C. Fischer, F. A. Mautner, N. Kulak and S. S. Massoud, *Eur. J. Inorg. Chem*., 2018, 2322-2338.

View Article Online
DOI: 10.1039/C9NJ00061E

41. W. Xu, J. A. Craft, P. R. Fontenot, M. Barens, K. D. Knierim, J. H. Albering, F. A. Mautner and S. S. Massoud, *Inorg. Chim. Acta,* 2011, **373**, 159-166.

42. A. W. Addison, T. N. Rao, J. Reedijk, J. V. Rijin and G. C. Verschoor, *J. Chem. Soc., Dalton Trans.*, 1984, 1349-1356.

43. H. Nagao, N. Komeda, M. Mukaida, M. Suzuki and K. Tanaka, *Inorg. Chem.*, 1996, **35**, 6809-6815.

44. W. J. Geary, *Coord. Chem. Rev.*, 1971, **7**, 81-122.

45. B. J. Hathaway BJ, in G. Wilkinson, R. D. Gillard and J. A. McCleverty (Eds), in Comprehensive Coordination Chemistry, vol. 5, Pergamon, Press, Oxford, England, 1987, pp. 533

46. F. A. Mautner, K. N. Landry, A. A. Gallo and S. S. Massoud, *J. Mol. Struct.*, 2007, **837**, 72-78.

47. S. S. Massoud, L. Le Quan, K. Gatterer, J. H. Albering, R. C. Fischer and F. A. Mautner, *Polyhedron*, 2012, **21**, 601-606.

48. F. A. Mautner, R. C. Fischer, L. G. Rashmawi, F. R. Louka and S. S. Massoud, *Polyhedron*, 2017, **124**, 237-242.

49. S. S. Massoud, F. R. Louka, R. N. David, M. J. Dartez, Q. L. Nguyn, N. J. Labry, R. C. Fischer and F. A. Mautner, *Polyhedron*, 2015, **90**, 258-265.

50. Z. Trávníček, J. Vančo, J. Hošek, R. Buchtík and Z. Dvořák, *Chem. Centr. J.*, 2012, **6**, article number 160. doi:10.1186/1752-153X-6-160.

51. C. Santini, M. Pellei, V. Gandin, M. Porchia, F. Tisato and C. Marzano, *Chem. Rev.*, 2014, **114**, 815−862.

52. S. S. Massoud, C. C. Ledet, T. Junk, S. Bosch, P. Comba, R. Herchel, J. Hošek, Z. Trávníček, R. C. Fischer and F. A. Mautner, *Dalton Trans.* 2016, 45, 12933-12950.

53. V. G. Vaidyanathan and B. U. Nair, *Inorg. Biochem.*, 2003, 93271–93276.

54. M. L. Kremer, *Phys Chem Chem Phys.*, 1999, **1**, 3595-3605.

55. T. Osako, S. Nagatomo, T. Kitagawa, C. J. Cramer and S. Itoh, *J. Biol. Inorg. Chem.*, 2005, **10**, 581–590.

56. B. Bissaro, Å. K. Røhr, G. Müller, P. Chylenski, M. Skaugen, Z. Forsberg, S. J. Horn, G. Vaaje-Kolstad and V. G. H. Eijsink, *Nat. Chem. Biol*., 2017, **13**, 1123-1128.

View Article Online
DOI: 10.1039/C9NJ00061E

57. L. Ciano, G. J. Davies, W. B. Tolman and P. H. Walton, *Nature Catalysis*, 2018, **1**, 571–577.

58. Bruker (2005) SAINT v. 7.23; Bruker (2006) APEX 2,v. 2.0-2; Bruker AXS Inc. Madison, Wisconsin, USA.

59. G. M. Sheldrick, 2001, SADABS v. 2. University of Goettingen, Germany.

60. G. M. Sheldrick, *Acta Crystallogr.,* 2008, **A64**, 112-122.

61. G. M. Sheldrick, *Acta Crystallogr.,* 2015, **C71**, 3-8.

62. C. F. Macrae, P. R. Edington, P. McCabe, E. Pidcock , G. P. Shields, R. Taylor, T. Towler and J. van de Streek, *J. Appl. Cryst.,* 2006, **39**, 453-457.

63. M. Bancirova, *Luminescence*, 2011, **26**, 685-688.

64. J. E. Repine, J. W. Eaton, M. W. Anders, J. R. Hoidal and R. B. Fox, *J. Clin. Invest.*, 1979, **64**, 1642-1651.

View Article Online
DOI: 10.1039/C9NJ00061E

Graphical Abstract & Synopsis

Copper(II) complexes based on tripodal pyridyl amine derivatives as efficient anticancer agents

Salah S. Massoud,[*a] Febee R. Louka,[a] Ada F. Tusa,[a] Nicole E. Bordelon,[a] Roland C. Fischer,[b] Franz A. Mautner,[*c] Ján Vančo,[d] Jan Hošek,[d] Zdeněk Dvořák[d] and Zdeněk Trávníček[*d]

The *in vitro* cytotoxicity of a series of chlorido-Cu(II) complexes based on tripod pyridyl *N4*-donors derivatives revealed significant-to-moderate cytotoxicity against human cancer cell lines with best results obtained for $[Cu(BQPA)Cl]ClO_4/PF_6$ (**5-ClO_4/PF_6**) with IC_{50} values of 4.7–10.8 μM.